

Shear-Alfvén waves in gyrokinetic plasmas

W. W. Lee, J. L. V. Lewandowski, T. S. Hahm, and Z. Lin

Plasma Physics Laboratory, Princeton University, Princeton, New Jersey 08543

(Received 8 January 2001; accepted 3 July 2001)

It is found that the thermal fluctuation level of the shear-Alfvén waves in a gyrokinetic plasma is dependent on plasma β ($\equiv c_s^2/v_A^2$), where c_s is the ion acoustic speed and v_A is the Alfvén velocity. This unique thermodynamic property based on the fluctuation–dissipation theorem is verified in this paper using a new gyrokinetic particle simulation scheme, which splits the particle distribution function into the equilibrium part as well as the adiabatic and nonadiabatic parts. The numerical implication of this property is discussed. © 2001 American Institute of Physics.
[DOI: 10.1063/1.1400124]

I. INTRODUCTION

Gyrokinetic particle simulation^{1,2} was developed for the purpose of reducing the temporal and spatial disparities in the simulation plasma when one is only interested in the long-wavelength and low-frequency modes in magnetically confined plasmas. Another benefit of the gyrokinetic approach is the reduction of the numerical noise in the simulation.^{2,3} With the introduction of the perturbative (δf) particle simulation scheme,⁴ numerical noise is no longer an issue, because we can always make it arbitrarily small.⁵ However, in this paper, we will show that the noise issue is still relevant for perturbative gyrokinetic particle simulation when finite- β effects associated with shear-Alfvén physics are important. Both analytic and numerical results will be presented. The former is based on the usual fluctuation–dissipation theorem and the latter uses a new simulation scheme which is the finite- β extension of the split-weight perturbative gyrokinetic particle simulation scheme in the electrostatic approximation.⁶ Specifically, the new split-weight scheme breaks up the distribution function into an equilibrium part, F_0 , as well as an adiabatic part and a nonadiabatic part. The adiabatic part is associated with the product of F_0 and the effective potential of $\psi = \phi + \int \partial A_{\parallel} / c \partial t dx_{\parallel}$, and the nonadiabatic part is followed dynamically. Here, ϕ is the electrostatic potential, A_{\parallel} is the vector potential, and x_{\parallel} is the spatial coordinate along the field line. As we will discuss, without the use of ψ , numerical noise can interfere with the formation of shear-Alfvén normal modes. The present paper is organized as follows. In Sec. II, the basic finite- β gyrokinetic formulation based on the generalized Ohm's law is described. The theoretical properties in terms of the effective potential, ψ , are discussed in Sec. III. The finite- β split-weight scheme and its use for the verification of the numerical properties are given in Secs. IV and V, respectively.

II. FINITE- β GYROKINETICS AND THE GENERALIZED OHM'S LAW

In the gyrokinetic units of ρ_s ($\equiv \sqrt{\tau} \rho_i$) and Ω_i^{-1} for length and time, respectively, the governing gyrokinetic Vlasov equation for a finite- β plasma in slab geometry in the limit of $k_{\perp}^2 \rho_i^2 \ll 1$ can be written as⁷

$$\begin{aligned} \frac{dF_{\alpha}}{dt} \equiv \frac{\partial F_{\alpha}}{\partial t} + v_{\parallel} \hat{\mathbf{b}} \cdot \frac{\partial F_{\alpha}}{\partial \mathbf{x}} - \nabla \phi \times \hat{\mathbf{b}}_0 \cdot \frac{\partial F_{\alpha}}{\partial \mathbf{x}} \\ + s_{\alpha} v_{i\alpha}^2 \frac{\partial \psi}{\partial x_{\parallel}} \frac{\partial F_{\alpha}}{\partial v_{\parallel}} = 0, \end{aligned} \quad (1)$$

where $\tau \equiv T_e / T_i$, α denotes species, $v_{ie}^2 = m_i / m_e$, $v_{ii}^2 = 1 / \tau$, $s_e = 1$, $s_i = -\tau$,

$$\hat{\mathbf{b}} \equiv \hat{\mathbf{b}}_0 + \frac{\delta \mathbf{B}}{B_0} = \frac{\mathbf{B}_0}{B_0} + \nabla A_{\parallel} \times \hat{\mathbf{b}}_0, \quad (2)$$

$$\mathbf{E}^L = -\nabla \phi, \quad E_{\parallel}^T = -\frac{\partial A_{\parallel}}{\partial t}, \quad (3)$$

and the superscripts L (ongitudinal) and T (ransverse) denote the decomposition relative to the direction of wave propagation. The effective potential in Eq. (1) is defined as

$$\frac{\partial \psi}{\partial x_{\parallel}} \equiv -(\mathbf{E}^L + E_{\parallel}^T \hat{\mathbf{b}}_0) \cdot \hat{\mathbf{b}} = \frac{\partial \phi}{\partial x_{\parallel}} + \frac{\partial A_{\parallel}}{\partial t}, \quad (4)$$

and $\partial / \partial x_{\parallel} \equiv \hat{\mathbf{b}}_0 \cdot \nabla$. The gyrokinetic Poisson's equation for $k_{\perp}^2 \rho_i^2 \ll 1$ can be simplified as

$$\nabla_{\perp}^2 \phi = \int (F_e - F_i) dv_{\parallel}, \quad (5)$$

where the electrostatic potential ϕ is normalized by T_e / e and $\int F_{0\alpha} dv_{\parallel} = 1$. Ampere's law then becomes

$$\nabla_{\perp}^2 A_{\parallel} = \beta \int v_{\parallel} (F_e - F_i) dv_{\parallel}, \quad (6)$$

where the vector potential A_{\parallel} is normalized by $c T_e / e c_s$, $\beta \equiv c_s^2 / v_A^2$, $v_A \equiv c \lambda_D / \rho_s$ is the Alfvén speed, and λ_D is the electron Debye length. [Note that the ion acoustic speed c_s ($\equiv \rho_s \Omega_i$) is unity in the gyrokinetic unit.] Equations (1)–(6) are the so-called (electromagnetic) Darwin model, in which the transverse induction electric current, $\partial \mathbf{E}^T / \partial t$, is neglected in Ampere's law. The approximation of $J_{\parallel}^T \approx J_{\parallel}$ valid for $k_{\parallel} \ll k_{\perp}$ is also used here. To expedite the calculation of $\partial \psi / \partial x_{\parallel}$ of Eq. (4), a generalized Ohm's law in shearless slab geometry, by combining Eqs. (1)–(6), can be written as

$$\begin{aligned} & \left[\nabla_{\perp}^2 - \beta \left(\frac{m_i}{m_e} \int F_e dv_{\parallel} + \int F_i dv_{\parallel} \right) \right] \frac{\partial \psi}{\partial x_{\parallel}} \\ &= \beta \frac{\partial}{\partial x_{\parallel}} \int v_{\parallel}^2 (F_i - F_e) dv_{\parallel} - \beta \nabla \phi \\ & \quad \times \hat{\mathbf{b}}_0 \cdot \nabla \int v_{\parallel} (F_i - F_e) dv_{\parallel} - \frac{\partial}{\partial x_{\parallel}} \int (F_i - F_e) dv_{\parallel}. \end{aligned} \quad (7)$$

The present paper represents the first attempt to study the properties of the generalized potential, ψ , in both theory and simulation based on Eq. (7). The use of this equation for shear-Alfvén physics was first suggested in Ref. 8.

III. THEORETICAL PROPERTIES OF FINITE- β GYROKINETIC PLASMAS

Starting from Eq. (1) and using $F_{\alpha} = F_{0\alpha} + \delta f_{\alpha}$ and $\partial F_{0\alpha} / \partial t + v_{\parallel} \hat{\mathbf{b}}_0 \cdot \partial F_{0\alpha} / \partial \mathbf{x} = 0$, we obtain

$$\frac{d \delta f_{\alpha}}{dt} = - \frac{d F_{0\alpha}}{dt} = s_{\alpha} v_{\parallel} \frac{\partial \psi}{\partial x_{\parallel}} F_{0\alpha}, \quad (8)$$

where d/dt is defined in Eq. (1) and the zeroth-order inhomogeneity is ignored. The generalized Ohm's law, Eq. (7), should then be changed accordingly as

$$\begin{aligned} & \left[\nabla_{\perp}^2 - \beta \frac{m_i}{m_e} \right] \frac{\partial \psi}{\partial x_{\parallel}} = \beta \frac{\partial}{\partial x_{\parallel}} \int v_{\parallel}^2 (\delta f_i - \delta f_e) dv_{\parallel} \\ & \quad - \frac{\partial}{\partial x_{\parallel}} \int (\delta f_i - \delta f_e) dv_{\parallel}, \end{aligned} \quad (9)$$

where the higher order nonlinear terms have been dropped. The theoretical and numerical properties of the shear-Alfvén waves can be studied as follows. The linearized version of Eq. (8),

$$\frac{\partial \delta f_{\alpha}}{\partial t} + v_{\parallel} \frac{\partial \delta f_{\alpha}}{\partial x_{\parallel}} = s_{\alpha} v_{\parallel} \frac{\partial \psi}{\partial x_{\parallel}} F_{0\alpha}, \quad (10)$$

with the ansatz of $\exp(ik_{\parallel}x_{\parallel} - i\omega t)$ gives

$$\delta f_{\alpha} = \left(1 + \frac{\omega}{k_{\parallel} v_{\parallel} - \omega} \right) s_{\alpha} F_{0\alpha} \psi. \quad (11)$$

Substituting it into Eq. (9), we obtain the dispersion relation as

$$D \equiv \frac{1}{k^2 \lambda_D^2} \left[k_{\perp}^2 + \left(1 - \beta \frac{\omega^2}{k_{\parallel}^2} \right) [\tau(1 + X_i) + (1 + X_e)] \right] = 0, \quad (12)$$

where D is the dielectric constant for $k^2 \lambda_D^2 \ll 1$ and

$$X_{\alpha} \equiv \frac{\omega}{\sqrt{2} k_{\parallel} v_{i\alpha}} Z \left(\frac{\omega}{\sqrt{2} k_{\parallel} v_{i\alpha}} \right).$$

For the cold response of $\omega \gg k_{\parallel} v_{i\alpha}$, Eq. (12) gives the normal modes as

$$\omega = \pm \frac{\omega_H}{\sqrt{1 + \omega_{pe}^2 / c^2 k^2}} = \pm \frac{k_{\parallel} v_A}{\sqrt{1 + c^2 k^2 / \omega_{pe}^2}}, \quad (13)$$

where $c / \omega_{pe} (\equiv \rho_s \sqrt{m_e / m_i \beta})$ is the electron skin depth. In the electrostatic limit of $\omega_{pe}^2 / c^2 k^2 \rightarrow 0$, it recovers the shear-Alfvén modes in the electrostatic limit, i.e., $\omega_H [\equiv (k_{\parallel} / k_{\perp}) \sqrt{m_i / m_e} \Omega_i]$ as discussed in Ref. 2. Equation (13), valid for $\beta \ll m_e / m_i$, shows that the magnitude of the shear-Alfvén frequencies becomes lower for higher β 's. For the warm electron response of $\omega \ll k_{\parallel} v_{te}$, the oscillation frequencies from Eq. (12) become

$$\omega = \pm k_{\parallel} v_A \sqrt{1 + k_{\perp}^2}, \quad (14)$$

and the corresponding damping rate is

$$\frac{\gamma}{\omega} = - \frac{1}{2} \sqrt{\frac{\pi}{\beta}} \frac{\omega}{k_{\parallel} v_{te}} \frac{k_{\perp}^2}{1 + k_{\perp}^2}, \quad (15)$$

where $v_A \equiv \sqrt{1/\beta}$ is the Alfvén velocity. These are the usual kinetic shear-Alfvén waves for $\beta \gg m_e / m_i$ and both the magnitude of the frequency and the damping rate continue to decrease for higher β 's. For $\beta = 1$, the normal modes are $\omega = \pm k_{\parallel} c_s \sqrt{1 + k_{\perp}^2}$.

The total thermal fluctuation level in a finite- β gyrokinetic plasma is the consequence of integrating over the whole ω spectra of the fluctuation-theorem,³ i.e.,

$$V k^2 |\Psi(\mathbf{k})|^2 / 8\pi = \frac{T}{2} \left(\frac{1}{D(\omega = \infty)} - \frac{1}{D(\omega = 0)} \right) = \frac{T_e \lambda_D^2}{2 \rho_s^2}, \quad (16)$$

for $\tau = 1$, where $\Psi \equiv \int \psi d\omega$, D is given by Eq. (12), and V is the volume of the system. The corresponding fluctuation potential becomes

$$\left| \frac{e \Psi}{T_e} \right| = \frac{1}{\sqrt{N} k \rho_s}, \quad (17)$$

where N is the number of simulation particles in the waves with the wave number k . These levels resemble those in terms of \mathbf{E}^L or ϕ obtained earlier for finite- β plasmas^{9,10} as well as those for the electrostatic cases.^{2,3} Thus, there is no reduction in the total noise level due to finite β effects. The troublesome aspect of this result is that the noise level is greatly enhanced for long wavelength modes with $k \rho_s \ll 1$. However, as we will show, the fraction of this noise that resides in the shear-Alfvén normal modes actually decreases with β . To proceed, let us again use ψ in Eq. (9). Starting from the fluctuation-dissipation theorem,¹¹ we can express the thermal fluctuation level for the normal modes of interest as

$$V k^2 |\psi(\mathbf{k})|^2 / 8\pi = \frac{T_e}{2} \sum_{\Omega} \frac{1}{|\omega \partial D_R / \partial \omega|_{\Omega}}, \quad (18)$$

where D_R is the real part of the dielectric constant, Eq. (12), and Ω is the normal mode. For the cold electron response of $\omega \gg k_{\parallel} v_{te}$ and from Eq. (13), we obtain

$$V k^2 |\psi(\mathbf{k})|^2 / 8\pi = \frac{T_e \lambda_D^2}{2 \rho_s^2} \frac{1}{1 + \omega_{pe}^2 / c^2 k^2}, \quad (19)$$

and, correspondingly,

$$\left| \frac{e\psi}{T_e} \right| = \frac{1}{\sqrt{N}k\rho_s} \frac{1}{\sqrt{1 + \omega_{pe}^2/c^2k^2}}. \quad (20)$$

Apparently, there is reduction in the noise level as shown in Eq. (20) due to finite- β effects. Equations (19) and (20) are valid for $\beta \ll m_e/m_i$. In the limit of $\beta=0$ ($\psi \rightarrow \phi$), we recover the level of $|e\phi/T_e| = 1/\sqrt{N}k\rho_s$ as given by Refs. 2 and 3. For the warm electron response of $\omega \ll k_{\parallel}v_{te}$, Eq. (18) gives

$$Vk^2|\psi(\mathbf{k})|^2/8\pi = \frac{T_e}{2} \frac{k^2\lambda_D^2}{1+k^2\rho_s^2}, \quad (21)$$

by using Eq. (14) and, in turn, the noise level becomes

$$\left| \frac{e\psi}{T_e} \right| = \frac{1}{\sqrt{N}} \frac{1}{\sqrt{1+k^2\rho_s^2}}. \quad (22)$$

Thus, Eqs. (21) and (22) indicate that, for $\beta > m_e/m_i$, the noise level is much reduced and is nearly constant for $k_{\perp}^2\rho_s^2 \ll 1$. For $\beta=0$ with warm electrons and cold ions, Eq. (12) gives the normal mode of $\omega = \pm k_{\parallel}c_s/\sqrt{1+k^2\rho_s^2}$, which is the gyrokinetic version of the ion acoustic waves and its thermal energy and noise level are the same as those given in Eqs. (21) and (22) with ψ replaced by ϕ . For $k^2\rho_s^2 \ll 1$, we recover the noise level for the usual ion acoustic waves. Thus, these results give the first conclusive evidence of the favorable trend for the numerical noise. Specifically, comparing them with Eqs. (16) and (17), it is evident that most of the numerical noise resides outside the normal modes for finite- β plasmas for $k_{\perp}\rho_s \ll 1$, while all the noise is in the normal modes for $\beta=0$. As we will show, the elimination of the unwanted noise is essential for simulating shear-Alfvén waves of $k_{\perp}^2\rho_s^2 \ll 1$ and, moreover, finite- β effects are even helpful numerically for the case of $k_{\perp}^2\rho_s^2 \sim 1$. The reasons that the total noise remains unchanged and that more noise resides outside the normal modes for higher β plasmas are due to the fact that, in gyrokinetic plasmas, the electrostatic normal modes, $\pm\omega_H$, which can interact with the noise generated by the fast particles, change into shear-Alfvén waves with phase velocities less than the electron thermal velocity for $\beta > m_e/m_i$. As such, there is no mechanism to damp out the noise generated by the fast particles and the total noise level remains the same regardless of β .

The interest in utilizing the desirable numerical properties of shear-Alfvén waves for simulation purposes was first mentioned in Ref. 8. However, a simple application of the perturbative δf scheme⁴ to solve Eqs. (8) and (9) was limited to low β plasmas, i.e., $\beta \ll m_e/m_i$.⁹ The subsequent work¹² using the canonical momentum as a phase space variable⁷ had to use a total f code to produce shear-Alfvén waves. We believe that, in both cases, numerical noise causes the problem, i.e., the interference of the nonadiabatic responses of the fast electrons with the collective oscillations of shear-Alfvén waves is the culprit.

IV. THE SPLIT-WEIGHT SCHEME FOR FINITE- β PLASMAS

To prove this point numerically, we have devised a new simulation scheme, which is the extension of the split-weight δf scheme⁶ to finite- β plasmas. Briefly, the scheme divides the perturbed electron distribution into the adiabatic and nonadiabatic parts, i.e.,

$$\delta f_e = \psi F_{0e} + \delta h_e.$$

From $d\psi/dt = \partial\psi/\partial t + v_{\parallel}\hat{\mathbf{b}} \cdot \partial\psi/\partial \mathbf{x} - \nabla\phi \times \hat{\mathbf{b}}_0 \cdot \partial\psi/\partial \mathbf{x}$ and Eq. (1), and dropping the nonlinear terms, we obtain

$$\frac{d\delta h_e}{dt} = -\frac{\partial\psi}{\partial t}F_{0e}. \quad (23)$$

Defining

$$w^{\text{NA}} \equiv \delta h_e/F_e,$$

the weight equation can then be written as

$$\frac{dw^{\text{NA}}}{dt} = \frac{1}{F_e} \frac{d\delta h_e}{dt} = -\frac{1-w^{\text{NA}}}{1+\psi} \frac{\partial\psi}{\partial t}. \quad (24)$$

The corresponding equations of motion are

$$\frac{d\mathbf{x}}{dt} = v_{\parallel}\hat{\mathbf{b}}_0 - \nabla(\phi - v_{\parallel}A_{\parallel}) \times \hat{\mathbf{b}}_0, \quad (25)$$

$$\frac{dv_{\parallel}}{dt} = s_{\alpha}v_{i\alpha}^2 \frac{\partial\psi}{\partial x_{\parallel}}, \quad (26)$$

and the generalized Ohm's law is simplified as

$$\begin{aligned} (\nabla_{\perp}^2 - 1) \frac{\partial\psi}{\partial x_{\parallel}} &= \beta \frac{\partial}{\partial x_{\parallel}} \int v_{\parallel}^2 (\delta f_i - \delta h_e) dv_{\parallel} \\ &\quad - \frac{\partial}{\partial x_{\parallel}} \int (\delta f_i - \delta h_e) dv_{\parallel}, \end{aligned} \quad (27)$$

where the perturbed ion distribution can be calculated by the standard δf scheme⁴ with

$$\delta f_i = \sum_{j=1}^N w_j \delta(\mathbf{x} - \mathbf{x}_j) \delta(v_{\parallel} - v_{\parallel j})$$

and the nonadiabatic electron contribution is given by

$$\delta h_e = \sum_{j=1}^N w_j^{\text{NA}} \delta(\mathbf{x} - \mathbf{x}_j) \delta(v_{\parallel} - v_{\parallel j}).$$

Taking $\partial/\partial t$ of Eqs. (9) and (27) and using Eqs. (8) and (23), we arrive at

$$\begin{aligned} \left[\nabla_{\perp}^2 - \beta \frac{m_i}{m_e} \right] \frac{\partial\psi}{\partial t} &= -\beta \frac{\partial}{\partial x_{\parallel}} \int v_{\parallel}^3 (\delta f_i - \delta h_e) dv_{\parallel} \\ &\quad + \frac{\partial}{\partial x_{\parallel}} \int v_{\parallel} (\delta f_i - \delta h_e) dv_{\parallel}. \end{aligned} \quad (28)$$

Equations (24)–(28) form the basic set for finite- β split-weight particle simulation. We should remark here that the dispersion relation, Eq. (12), which is the basis for the theo-

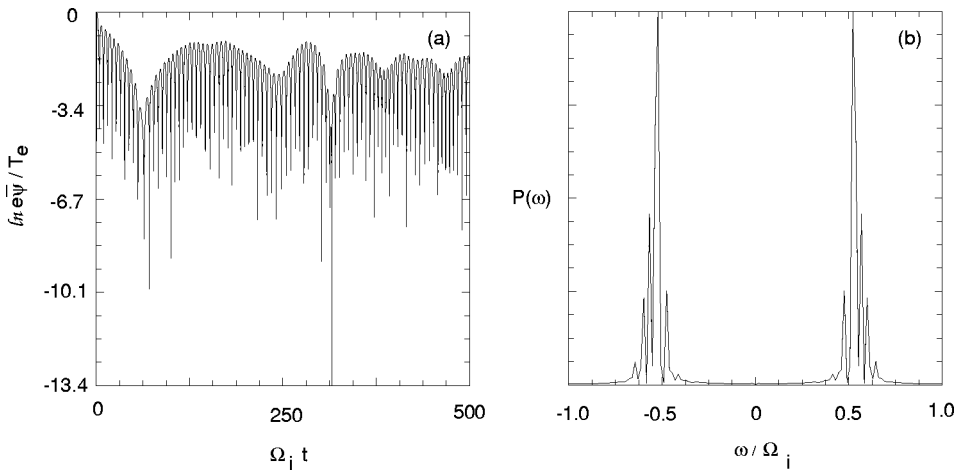


FIG. 1. (a) Damping rate and noise level, and (b) frequencies for the shear-Alfvén waves for $\beta=0.0\%$.

retical properties presented in Sec. III, can easily be recovered by using Eqs. (23) and (28) together with the necessary equations for the ion response.

V. FINITE- β GYROKINETIC PARTICLE SIMULATION RESULTS

The simulation has been carried out with a one-dimensional simulation with quiet start code, GK1D.^{4,6} In the code, both x and z are ignorable coordinates, $y = \theta x_{\parallel}$, and $\theta \ll 1$ is the angle between the external B field and the z axis. This is a linear simulation in which Eqs. (24)–(26) are simplified to

$$dx_{\parallel}/dt = v_{\parallel}, \quad dv_{\parallel}/dt = 0,$$

and

$$dw^{\text{NA}}/dt = -\partial\psi/\partial t,$$

respectively.

The simulation uses a 64 grid system with 6765 particles and includes only the modes with $k\rho_s \approx \pm 0.4$. The other parameters are: $m_i/m_e = 1837$, $\tau = 1$, $\theta = 0.01$, and a (particle size) = 0. In all the simulations reported here, we initialized the system with $w_j \ll 1$ for the ions and $w_j^{\text{NA}} \ll 1$ for the electrons. The properties of the resulting $\bar{\psi}[\equiv \psi(t)/\psi(t=0)]$ in terms of the fluctuation (noise) level, damping rate, and frequency (based on the whole time history) for $\beta=0$ are

shown in Fig. 1, where $\Omega_i \Delta t = 0.2$ is the time step used in the simulation for resolving these modes. These are the well-known ω_H modes, which have first been studied in detail and well understood in Ref. 2. The noise level of $e\bar{\psi}/T_e \approx 3\%$ is reached at $\Omega_i t = 60$. However, the noise fluctuates wildly in the ensuing simulation and reaches as high as 20% at times. These high amplitude oscillations are mainly due to the lack of simulation particles at the Maxwellian tail of $\omega/k_{\parallel} \approx 2.5v_{te}$. The simulation frequencies of $\omega/\Omega_i = \pm 0.51$ shown in Fig. 1 are higher than the theoretical values of $\omega/\Omega_i = \pm 0.43$ given by Eq. (13) again due to the enhanced noise as well as the high damping rate which tends to broaden the frequency spectrum. These discrepancies in amplitude and frequency can, of course, be improved with more particles. But, as we will show, they can also be improved with the finite- β effects without using more particles. For example, for the case of $\beta=0.01\%$ with the same number of particles and the same time step, the measured frequencies become ± 0.32 compared favorably with the theoretical value of ± 0.3 from Eq. (13). As shown in Fig. 2 for the case of $\beta=0.1\%$ where again the same number of particles are used, but with a larger time step of $\Omega_i \Delta t = 2$, both the linear frequencies (based on the whole time history) and the damping rate of $(\omega + i\gamma)/\Omega_i = \pm 0.13 - i0.011$ are in excellent agreement with the theoretical predictions of $\pm 0.14 - i0.011$ from Eqs. (14) and (15). In the steady state, the

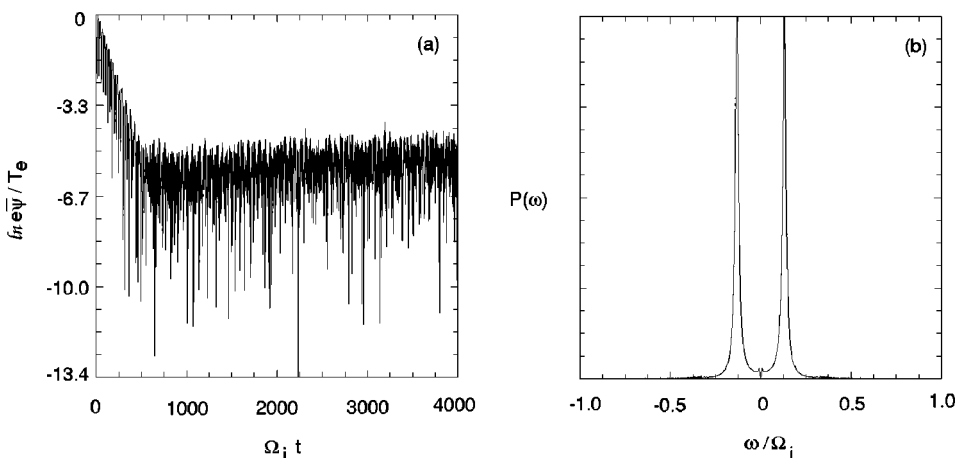


FIG. 2. (a) Damping rate and noise level, and (b) frequencies for the shear-Alfvén waves for $\beta=0.1\%$.

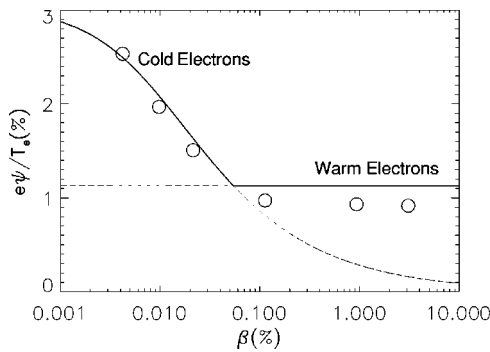


FIG. 3. Comparisons of fluctuation levels between simulations and theoretical predictions.

noise level reaches $e\bar{\psi}/T_e \approx 1.0\%$, without any numerical enhancement. To compare these fluctuation levels to the theoretical predictions by Hu and Krommes,⁵ let us renormalize the steady-state values for ψ in Figs. 1 and 2 by the average particle weight of $\bar{w} \equiv \sqrt{\sum (w_{NA})^2} / N/2$ in the corresponding steady state. We then obtain $(e\psi/T_e)/\bar{w} \approx 8.0\%$ and 1.0% for $\beta=0$ and 0.1% , respectively. The corresponding fluctuation levels are 3.0% and 1.2% , calculated, respectively, from Eqs. (20) and (22). The former is in the cold electron limit and the noise enhancement due to lack of particles is evident. The latter is already in the warm electron limit for a nominal β and the agreement is excellent. We have also studied the cases of $\beta=0.004\%$, 0.01% , 0.02% , 1.0% , and 3% , and their linear properties in terms of frequencies and growth rates agree well with the theoretical values. Their time-averaged fluctuations in the steady state are also in excellent agreement with theory based on Eqs. (20) or (22) as shown in Fig. 3, where $e\psi/T_e$ is normalized to \bar{w} . Note that the total fluctuation level for the simulation should be about 3% as predicted by Eq. (17) for these cases and it is 2.5 times higher than the noise residing in the shear-Alfvén waves for the warm electrons with $k\rho_s=0.4$ as given by Eq. (22). Thus, the split-weight scheme correctly keeps the noise associated with the normal modes while, effectively, eliminating the noise outside of them. For $\beta=10\%$ and $\Omega_i\Delta t=2$, the frequencies and the damping rate of $(\omega+i\gamma)/\Omega_i = \pm 0.014 - i0.00011$, as given by Fig. 4, are in excellent agreement with ± 0.014

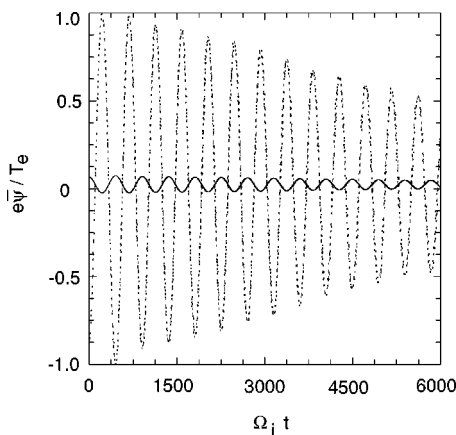


FIG. 4. Shear-Alfvén oscillations for $\beta=10.0\%$.

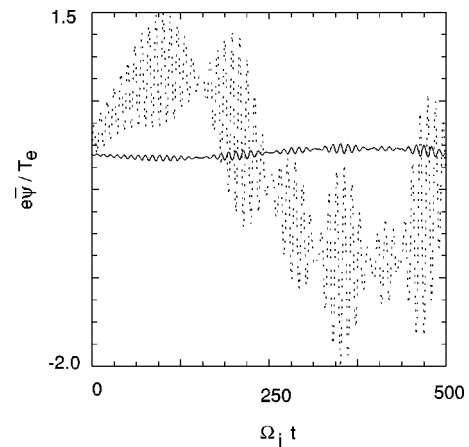


FIG. 5. Shear-Alfvén oscillations for $\beta=10.0\%$ including non-normal mode noise.

$-i0.00010$ predicted by theory. However, the fluctuation amplitude of 5% at the end of the simulation is considerably higher than the theoretical prediction. The difficulty here is that the damping rate is more than 100 times smaller than the real frequencies. As such, we have to use a very large number of time steps to reach the steady state. A very large number of time steps in a linearized collisionless simulation such as this means that we have to use sufficient number of particles to carry all the necessary phase space history information for all these time steps. Thus, we need more particles and more time steps to have a converged solution. Since we prefer to keep the same number of particles for all the cases presented here for comparison purposes, we will defer further discussions of these high- β cases to a later time. Nevertheless, the simulation data in Fig. 3 cover the relevant range of β 's for the tokamaks and serve the purpose of this paper as well.

For comparison with the $\beta=10\%$ case in Fig. 4, we have carried out a similar simulation by using the δf scheme based on Eqs. (8) and (9)⁴ with the same parameters. It is found that the simulation is numerically unstable. However, the stability is restored by using $\Delta t=0.2$. This is shown in Fig. 5. The excessive noise related to the tail distribution of the Maxwellian is evident, and the linear properties of the shear-Alfvén waves are substantially modified.

As for the time step for the warm electron cases, it is restricted by the parallel transit time requirement of $k_{\parallel}v_{te}\Delta t < 1$.² This complication is caused by the presence of the skin term, $\beta m_i/m_e$, on the left-hand side of Eq. (28), which needs to be canceled by the leading term from the v_{\parallel}^3 moment on the right-hand side to produce the correct response for $\omega/k_{\parallel}v_{te} \ll 1$. However, for $\omega/k_{\parallel}v_{te} \gg 1$, the skin term becomes dominant, e.g., near the rational surfaces, regardless of the plasma β . Therefore, it is an important term. Because of the absence of high frequency normal modes for a sufficiently high β plasma, one may use the adiabatic pushing scheme,¹³ in which one pushes electrons more often, to improve the situation. Specifically, by depositing the velocity moments for the electrons at every small time step, Δt , and push ions and solve field equations with a large time step, ΔT , one can use less electrons and, in turn, can effectively

circumvent the parallel Courant condition. The adiabatic pushing scheme described here is a time-explicit scheme. Therefore, it is an improved version of the orbit-averaged implicit particle scheme proposed earlier.¹⁴

VI. CONCLUSION

In conclusion, we believe that we have finally resolved a decade old puzzle concerning the favorable numerical trend for a finite- β gyrokinetic plasma,⁸ which is found here to be intimately related to the unique thermodynamic feature of the shear-Alfvén waves. Without such an understanding, one would conclude from Eq. (17)^{9,10} that finite- β gyrokinetic particle simulation of long wavelength modes with $k\rho_s \rightarrow 0$ is nearly impossible, because the noise is so much enhanced. On the other hand, the dramatic improvement of the noise property when increasing β from 0 to 0.1% for $k_\perp\rho_s \sim 1$ as shown in Figs. 1 and 2 highlights the important transition of the shielding effects from the ion polarization¹⁻³ to that of the adiabatic electrons. This transition can only be made apparent by the split-weight scheme. The usual δf scheme⁴ cannot detect this transition due to the interference of the numerical noise residing outside the normal modes. Most of all, we have developed a new simulation scheme that can be generalized to multidimensional simulations of finite- β plasmas.

ACKNOWLEDGMENTS

We would like to thank Dr. John A. Krommes for useful discussions. The research was supported by Contract No. DE-AC02-CHO-3073 and the Plasma Science Accelerated Computing Initiative of the U.S. DOE.

¹W. W. Lee, Phys. Fluids **26**, 556 (1983).

²W. W. Lee, J. Comput. Phys. **72**, 243 (1987).

³J. A. Krommes, W. W. Lee, and C. Oberman, Phys. Fluids **29**, 2421 (1986).

⁴S. E. Parker and W. W. Lee, Phys. Fluids B **5**, 77 (1993).

⁵G. Hu and J. A. Krommes, Phys. Plasmas **1**, 863 (1994).

⁶I. Manuilskiy and W. W. Lee, Phys. Plasmas **7**, 1381 (2000).

⁷T. S. Hahm, W. W. Lee, and A. Brizard, Phys. Fluids **31**, 1940 (1988).

⁸W. W. Lee, T. S. Hahm, and J. V. W. Reynders, Bull. Am. Phys. Soc. **34**, 2044 (1989).

⁹J. V. W. Reynders, Ph.D. thesis, Princeton University, 1992.

¹⁰J. A. Krommes, Phys. Rev. Lett. **70**, 3067 (1993); Phys. Fluids B **5**, 2405 (1993); **5**, 1066 (1993).

¹¹Yu. L. Klimontovich, *The Statistical Theory of Non-Equilibrium Processes in a Plasma* (MIT, Cambridge, 1967).

¹²J. C. Cummings, Ph.D. thesis, Princeton University, 1995.

¹³H. Qin, R. C. Davidson, and W. W. Lee, Phys. Rev. ST Accel. Beams **3**, 084401 (2000).

¹⁴B. I. Cohen, R. P. Freis, and V. Thomas, J. Comput. Phys. **45**, 345 (1982).